Wave-based active control for nonreciprocal acoustics using a planar array of secondary sources

Joe Tan[1]
University of Southampton
University Road, Southampton, SO17 1BJ

Jordan Cheer
University of Southampton
University Road, Southampton, SO17 1BJ

Steve Daley
University of Southampton
University Road, Southampton, SO17 1BJ

ABSTRACT

There has been significant interest in the design of nonreciprocal acoustic devices that allow acoustic waves to be perfectly transmitted in one direction, whilst the acoustic waves propagating in the opposite direction are blocked or reflected. Previously proposed nonreciprocal acoustic devices have broken the symmetry of transmission by introducing nonlinearities or resonant cavities. However, these nonreciprocal acoustic devices typically have limitations, such as signal distortions and the bandwidth over which nonreciprocal behaviour can be achieved is narrow. This paper will investigate how active control can be used to minimise the transmitted and reflected waves independently to achieve nonreciprocal sound transmission and absorption using a planar array of secondary sources in a two-dimensional environment. The advantage of the proposed active control system is that it is fully adaptable, which means that the directivity of nonreciprocal behaviour can also be reversed. The performance of the proposed wave-based active control system is investigated for a range of angles of incidence and its performance limitations are explored.

1. INTRODUCTION

Acoustic reciprocity is a fundamental property that is inherent in linear acoustic wave propagation, which describes the symmetry of sound transmission between two points. For example, the sound transmission between an acoustic source and observer is equal to the sound transmission when the acoustic source and observer are interchanged. In certain applications, acoustic reciprocity is not desirable, such as full duplex communication systems, which has led to significant interest in the development of nonreciprocal acoustic devices due to their ability to block or reflect wave propagation in one direction, whilst allowing the acoustic waves propagating in the opposite direction to be perfectly transmitted. Typically, these nonreciprocal acoustic devices achieve nonreciprocal sound transmission by introducing nonlinearities [1–3], fluid motion [4] or resonant cavities [5]. Since,

[1]j.tan@soton.ac.uk

linear nonreciprocal acoustic devices are usually based on the design of acoustic metamaterials, these devices can only achieve nonreciprocal behaviour over a narrow frequency range due to their reliance on passive resonators. Although, broadband nonreciprocal sound transmission has been achieved using nonlinear nonreciprocal acoustic devices [6], these systems typically have limitations, such as signal distortions and they are generally not fully adaptable because the directivity of the nonreciprocal behaviour is fixed due to the use of gain and loss media [7].

A variety of active nonreciprocal acoustic devices have been proposed [1,7], however, these active control systems are typically combined with passive resonators and, therefore, the passive resonators still limit the bandwidth that nonreciprocal behaviour can be achieved over. Therefore, this paper investigates how active control can be used to control the transmitted and reflected wave components individually to achieve nonreciprocal sound transmission and absorption in a two-dimensional environment using an infinite planar array of control sources. This paper is structured as the follows: Section 2 and 3 describe the system setup and wave separation method used in this paper. Section 4 describes the wave based active control formulations used to obtain the optimal control source strengths that minimise the transmitted and reflected wave components. Section 5 and 6 present the results of simulations and conclusions respectively.

2. SYSTEM DESCRIPTION

Figure 1 shows the system setup used in this paper to investigate how active can be used to achieve nonreciprocal sound transmission and absorption using an infinite array of control sources in a two-dimensional environment. From Figure 1 it can be seen that there are two primary incident plane waves, where one is propagating in the positive direction and the other is propagating in the negative direction as shown in Figure 1. The system shown in Figure 1 also contains an infinite length dual layer array of point monopole control sources located at the centre of the region with two infinite planar arrays of closely spaced pressure sensors positioned either side of the control sources. Figure 1 also shows the positive and negative propagating wave components, which are indicated by the coefficients A to D.

Two different active control strategies have been employed in this paper: a single layer of point monopole control sources that are driven to minimise the transmitted wave, C, and a dual layer of point monopole control sources that are driven to minimise the transmitted, C, and reflected, B, waves. The performance of the two considered active strategies will be investigated in two different scenarios: when the angle of incidence is normal (0° incidence) and oblique (45° incidence).

Table 1 shows the system parameters used in this paper for the simulations and these system parameters are also shown in Figure 1.

Table 1: System parameters used in this paper .

Variable	**Value**	**Variable**	**Value**
x_1	-0.9m	x_2	-0.8m
x_3	0.8m	x_4	0.9m
d_x	0.11m	d_y	0.39m
Δx	0.1m		

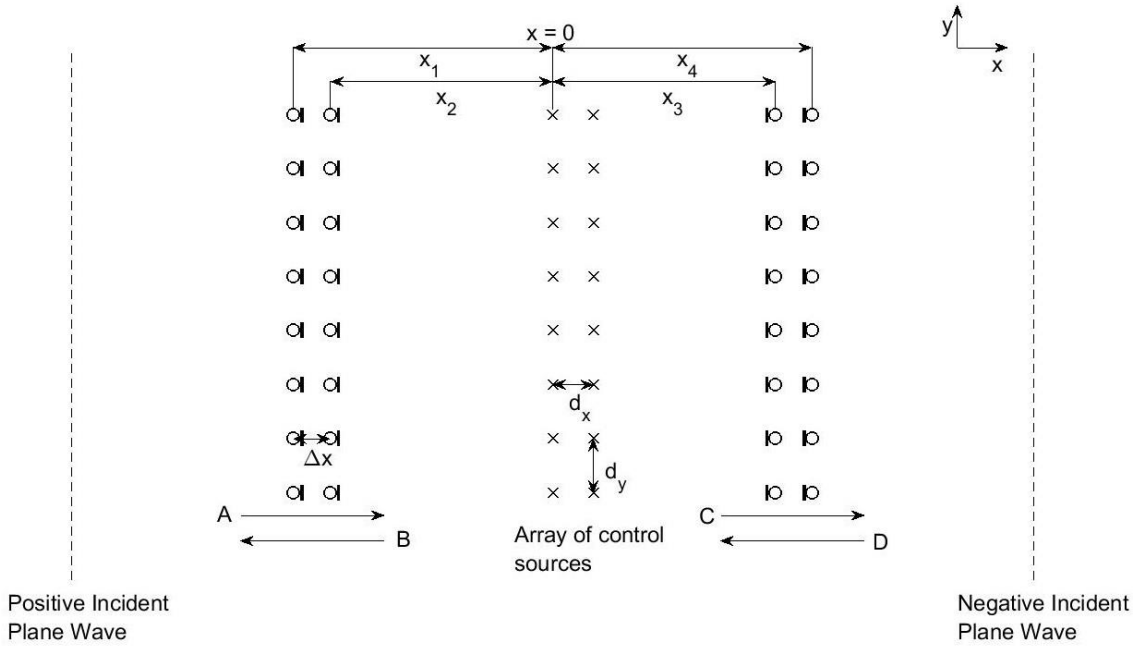

Figure 1: The system setup used in this paper to investigate how active control can be used to achieve nonreciprocal sound transmission and absorption using an infinite array of control sources in a two-dimensional environment.

3. WAVE SEPARATION METHOD

To control the transmitted and reflected waves individually, these wave components need to be separated from the total pressure measured using a wave separation method and a pair of closely spaced pressure sensors as shown in Figure 1. There are variety of wave separation methods that can be used to separate the positive and negative propagating waves in a two-dimensional environment, such as the equivalent source method [8, 9] and the delay method [10, 11]. However, in this work the wave separation method based on the spatial Fourier transform has been utilised because it is easy to implement for planar arrays. This wave separation method is the integration method, which is similar to the approach described in [12], however, it has been extended to 2D via a one-dimensional discrete spatial Fourier transform (DSFT). The spatial Fourier transform (SFT) can be used to transform the pressure measured at each pressure sensor into their plane wave components in the wavenumber domain [10]. In the two-dimensional case, the SFT can be expressed as

$$p(x, k_y) = \int_{-\infty}^{\infty} p(x, y) \mathrm{e}^{-\mathrm{j}k_y y} dy \tag{1}$$

where

$$k_y = k_0 \sin\theta, \tag{2}$$

which is the spatial frequency in the y direction, k_0 is the acoustic wavenumber and θ is the angle of incidence. In reality, it is not straightforward to implement the SFT given by Eq. 1. Thus, this paper has approximated the SFT given by Eq. 1 by weighting the pressure measured at several sampling points along the four planes of pressure sensors shown in Figure 1. The weighted measured pressure at the ith pressure sensor in each plane shown in Figure 1 can be expressed as

$$p(x_i, k_{y_i}) = p(x_i, y_i) W(y_i) \tag{3}$$

where

$$W(y_i) = \mathrm{e}^{\mathrm{j}k_y y}, \tag{4}$$

which is a weighting factor that applies the appropriate phase shift from the centre sampling point in each pressure sensor plane shown in Figure 1. To implement the weighting factors in the time domain controller, they have been modelled using finite impulse response (FIR) filters and these FIR filters have been designed using the *invfreqz* [13] function in Matlab, which is a least mean square fitting approach. The ideal impulse responses of the weighting factors that are given by Eq. 4 can be obtained by an inverse Fourier transform of Eq. 4, however, these impulse responses are non-casual. To ensure causality in the weighting factor responses, a modelling delay has been introduced, as previously proposed in [14], to the weighting factors given by Eq. 4 before modelling the FIR filters. After the measured pressure at each pressure sensor has been transformed into the wavenumber domain according to Eq. 3, each pair of pressure sensors can be used to calculate the positive and negative propagating wave components using the same wave separation method described in [12]. As summarised in [12], this wave separation method calculates the total pressure and the particle velocity at the midpoint between each pair of pressure sensors shown in Figure 1. Assuming the distance between the pair of pressure sensors is small compared to smallest acoustic wavelength, the total pressure, p_{12_i}, and particle velocity, u_{12_i}, at the midpoint can be calculated as

$$p_{12_i} = \frac{p_{1_i}W(y_i) + p_{2_i}W(y_i)}{2}, \tag{5}$$

$$u_{12_i} = \frac{1}{\Delta x}\int_0^{T_s} p_{1_i}W(y_i) - p_{2_i}W(y_i)\ dt \tag{6}$$

where c_0 is the speed of sound, Δx is the distance between the pair of pressure sensors as shown in Figure 1, T_s is the sampling time, p_{1_i} and p_{2_i} are the total pressures measured at the ith pressure sensor in the first ($x = -x_1$) and second ($x = -x_2$) plane of pressure sensors as shown in Figure 1. Using the total pressure and particle velocity given by Eqs. 5 and 6, the positive propagating incident, A_i, and reflected, B_i, wave components at the ith pair of pressure sensors can be calculated as

$$A_i = \frac{p_{1_i}W(y_i) + p_{2_i}W(y_i)}{4} + \frac{c_0}{\Delta x}\int_0^{T_s} p_{1_i}W(y_i) - p_{2_i}W(y_i)\ dt, \tag{7}$$

$$B_i = \frac{p_{1_i}W(y_i) + p_{2_i}W(y_i)}{4} - \frac{c_0}{\Delta x}\int_0^{T_s} p_{1_i}W(y_i) - p_{2_i}W(y_i)\ dt. \tag{8}$$

The wave separation method described in this section has also been applied to the third ($x = x_3$) and fourth ($x = x_4$) planes of pressure sensors shown in Figure 1 to calculate the transmitted, C_i and the negative propagating incident, D_i, wave components.

4. WAVE BASED CONTROL FORMULATIONS FOR NONRECIPROCAL ACOUSTICS

Once the transmitted and reflected waves have been calculated using the wave separation method described in Section 3, active control can then be used to control the calculated transmitted and reflected wave components independently and the active control formulations for the proposed wave-based active control systems will be described in this section. As mentioned in Section 2, two different active control strategies have been investigated in this paper: a single layer of point monopole control sources that are driven to minimise the transmitted wave and a dual layer of point monopole control sources that are driven to minimise the transmitted and reflected wave components. A multichannel feedforward filtered reference least mean squares (FxLMS) adaptive algorithm has been employed in both the considered active control systems to obtain the optimal control source strengths that minimise the transmitted and reflected wave components. In both cases, the reference signal for the FxLMS algorithms is the positive propagating incident wave component, A, which has been calculated via the wave separation method described in Section 3.

4.1. Nonreciprocal Transmission Control

A single layer of point monopole control sources shown in Figure 1 can be driven to minimise the transmitted wave. The vector of error signals in this case is the transmitted wave, which can be defined as

$$\mathbf{e}_T(n) = \mathbf{d}_T(n) + \mathbf{R}_T(n)\mathbf{w}_T(n) \tag{9}$$

where

$$\mathbf{e}_T(n) = \begin{bmatrix} e_{T_1}(n) & e_{T_2}(n) \dots e_{T_L}(n) \end{bmatrix}^T, \quad \mathbf{d}_T(n) = \begin{bmatrix} d_{T_1}(n) & d_{T_2}(n) \dots d_{T_L}(n) \end{bmatrix}^T, \tag{10}$$

$$\mathbf{w}_T(n) = \begin{bmatrix} w_{11_i}(n), & w_{12_i}(n), & w_{1K_i}(n), w_{2K_i}(n) \dots & w_{MK_i}(n) \end{bmatrix}^T \tag{11}$$

$$\mathbf{R}_T(n) = \begin{bmatrix} R_{T_1}(n) & R_{T_1}(n-1) & \dots & R_{T_1}(n-I-1) \\ R_{T_2}(n) & R_{T_2}(n-1) & \dots & R_{T_2}(n-I-1) \\ \vdots & \vdots & \ddots & \vdots \\ R_{T_L}(n) & R_{T_L}(n-1) & \dots & R_{T_L}(n-I-1) \end{bmatrix}, \tag{12}$$

$$d_{T_i}(n) = \frac{d_{3_i}(n)W(y_i) + d_{4_i}(n)W(y_i)}{4} + \frac{c_0}{2\Delta x}\int_0^{T_s} d_{3_i}(n)W(y_i) - d_{4_i}(n)W(y_i)\, dt \tag{13}$$

$$R_{T_i}(n) = \frac{R_{3_i}(n)W(y_i) + R_{4_i}(n)W(y_i)}{4} + \frac{c_0}{2\Delta x}\int_0^{T_s} R_{3_i}(n)W(y_i) - R_{4_i}(n)W(y_i)\, dt, \tag{14}$$

I is the number of tapped delays in the controller, $\mathbf{w}_T(n)$ is the vector of FIR control filter coefficients, K is the number of reference signals, M is the number of control sources, L is the number of error signals, $d_{3_i}(n)$ and $d_{4_i}(n)$ are the pressures measured at the ith pressure sensor due to the primary source in the third and fourth plane of pressure sensors as shown in Figure 1, $R_{3_i}(n)$ and $R_{4_i}(n)$ are the reference signals that have been filtered by the plant model responses between the pressures measured at the third and fourth plane of pressure sensors and the control source voltages, which have been modelled using FIR filters. The cost function in this case is the mean squared value of the transmitted wave, which can be given as

$$J(n) = \mathbf{e}^T(n)\mathbf{e}(n). \tag{15}$$

Taking the derivative of the cost function with respective to the vector of FIR control filter coefficients, the resulting gradient can be expressed as

$$\frac{\partial J(n)}{\partial \mathbf{w}_T(n)} = 2[\mathbf{R}_T^T(n)\mathbf{R}_T(n) + \mathbf{R}_T^T(n)\mathbf{d}_T(n)] = 2\mathbf{R}_T(n)\mathbf{e}_T(n). \tag{16}$$

Using the negative gradient according to Eq. 16, the FxLMS algorithm can be used to adapt the vector of FIR control filter coefficients to minimise the transmitted wave and the FxLMS algorithm in this case can be expressed as

$$\mathbf{w}_T(n+1) = \mathbf{w}_T(n) - \mu\mathbf{R}_T(n)\mathbf{e}_T(n) \tag{17}$$

where μ is the convergence coefficient.

4.2. Nonreciprocal Absorption Control

Extending the active control strategy described in the previous section, a dual layer of point monopole control sources can be driven to minimise the transmitted and reflected wave components. The vector of error signals in this case is the transmitted and reflected wave components, which can be defined as

$$\mathbf{e}(n) = \mathbf{d}(n) + \mathbf{R}(n)\mathbf{w}(n) \tag{18}$$

where

$$\mathbf{e}(n) = \begin{bmatrix} e_{T_1}(n) & e_{R_1}(n) & e_{T_2}(n) & e_{R_2}(n) \dots e_{T_L}(n) & e_{R_L}(n) \end{bmatrix}^T, \tag{19}$$

$$\mathbf{d}(n) = \begin{bmatrix} d_{T_1}(n) & d_{R_1}(n) & d_{T_2}(n) & d_{R_2}(n) \dots d_{T_L}(n) & d_{R_L}(n) \end{bmatrix}^T, \tag{20}$$

$$\mathbf{w}(n) = \begin{bmatrix} w_{11_i}(n), & w_{12_i}(n), & w_{1K_i}(n), w_{2K_i}(n) \dots & w_{MK_i}(n) \end{bmatrix}^T \tag{21}$$

$$\mathbf{R}(n) = \begin{bmatrix} R_{T_1}(n) & R_{T_1}(n-1) & \dots & R_{T_1}(n-I-1) \\ R_{R_1}(n) & R_{R_1}(n-1) & \dots & R_{R_1}(n-I-1) \\ R_{T_2}(n) & R_{T_2}(n-1) & \dots & R_{T_2}(n-I-1) \\ R_{R_2}(n) & R_{R_2}(n-1) & \dots & R_{R_2}(n-I-1) \\ \vdots & \vdots & \ddots & \vdots \\ R_{T_L}(n) & R_{T_L}(n-1) & \dots & R_{T_L}(n-I-1) \\ R_{R_L}(n) & R_{R_L}(n-1) & \dots & R_{R_L}(n-I-1) \end{bmatrix}, \tag{22}$$

$$d_{R_i}(n) = \frac{d_{R_{1_i}}(n)W(y_i) + d_{R_{2_i}}(n)W(y_i)}{4} - \frac{c_0}{2\Delta x}\int_0^{T_s} d_{R_{1_i}}(n)W(y_i) - d_{R_{2_i}}(n)W(y_i)\, dt \tag{23}$$

$$R_{R_i}(n) = \frac{R_{R_{1_i}}(n)W(y_i) + R_{R_{2_i}}(n)W(y_i)}{4} - \frac{c_0}{2\Delta x}\int_0^{T_s} R_{R_{1_i}}(n)W(y_i) - R_{R_{2_i}}(n)W(y_i)\, dt, \tag{24}$$

$\mathbf{w}(n)$ are the vector of FIR control filter coefficients, $d_{1_i}(n)$ and $d_{2_i}(n)$ are the pressures measured at the ith pressure sensor due to the primary source in the first and second planes of pressure sensors as shown in Figure 1, $R_{1_i}(n)$ and $R_{2_i}(n)$ are the reference signals that have been filtered by the plant model responses between the pressures measured at the first and second planes of pressure sensors and the control source voltages. The cost function in this case is the mean squared value of the transmitted and reflected wave components and this can given by Eq. 15. Therefore, following the same procedure outlined in the previous section, the FxLMS algorithm for this active control system can be expressed as

$$\mathbf{w}(n+1) = \mathbf{w}(n) - \mu\mathbf{R}(n)\mathbf{e}(n). \tag{25}$$

5. RESULTS

This section presents the results of simulations when implementing the wave-based active control formulations described in Section 4. The performance of the two considered active control systems will be evaluated in terms of the transmission, reflection and absorption coefficients when the active control systems are subject to a positive and negative incident plane wave as shown in Figure 1. As mentioned in Section 2, the performance of the proposed active control strategies will also be evaluated at normal and oblique incidence.

5.1. Normal incidence

When the positive and negative propagating incident plane waves have an angle of incidence of 0°, the average performance metrics across the pairs of pressure sensors shown in Figure 1 have been calculated when implementing the two proposed wave-based active control systems and these results are shown in Figure 2. In the positive propagating incident wave case, Figure 2(a) shows that the single layer of point monopole control sources achieve zero transmission (blue line), which is the objective of this controller, and, thus, a proportion of the incident sound field is reflected (red line) and absorbed (black line) as shown in Figure 2(a). When the incident wave is propagating in the negative direction, Figure 2(b) shows that the single layer of point monopole control sources achieves perfect transmission with zero reflection and absorption. This is due to the fact that the reference signal, A for the transmitted wave controller described in Section 1, is zero and, therefore, there is no time advanced information for the transmitted wave controller, which leads to the normal incidence negative propagating wave being perfectly transmitted. Hence, the results presented in Figure 2

show that a single layer of point monopole control sources driven to minimise the transmitted wave achieves nonreciprocal sound transmission over the presented frequency range. It is worth noting that the transmitted wave controller described in Section 4 is fully adaptable since the directivity of the nonreciprocal behaviour can be reversed by changing the reference signal to the negative propagating incident wave, D, and the vector of error signals in this case is the wave component, B. Figure 2(c) shows that the absorption controller, described in Section 2, that drives the dual layer of point monopole control sources to achieve zero transmission and reflection and, thus, this leads to perfect absorption of the positive propagating incident wave. In the negative propagating incident wave case, the dual layer of point monopole control sources achieves perfect transmission with zero reflection and absorption. Similarly to the transmitted wave controller, when the absorption controller is subject to a negative propagating incident wave, the reference signals, A, are zero and, thus, the absorption controller does not control the transmitted and reflected wave components because it does not have any time advanced information. This figure also shows that this optimal driven dual layer of point monopole control sources also achieves nonreciprocal sound absorption. Similarly to the transmitted wave controller, the absorption controller is also fully adaptable because the directivity of the nonreciprocal behaviour can also be reversed. To provide further insight into the controller behaviour, Figure 3 shows the contour plots of the sound field generated by the normal incident positive propagating wave and the total sound field when implementing the proposed wave-based active control systems at 250Hz. Figure 3(a) shows the positive propagating normal incident wave without control. Figure 3(b) shows that the transmitted wave controller minimises the sound transmission, however, a proportion of the incident sound field is reflected at the control source boundary and amplifies the upstream sound field, which is consistent with the results presented in Figure 2(a). Figure 3(c) shows that the the sound field map for the absorption controller and it can be seen that, as designed, this minimises the sound transmission, but the sound field upstream of the control sources remains unchanged, since the reflection is also minimised.

5.2. Oblique incidence

In a two-dimensional environment, it is also important to evaluate the performance of the proposed wave-based active control systems when the positive and negative incident waves are propagating at an oblique angle and these results are shown in Figure 4. Similarly to the normal incident case shown in Figure 2, in the positive propagating incident wave case, the single layer of point monopole control sources achieves zero transmission with a proportion of the incident sound being reflected and absorbed. Conversely, when the incident wave is propagating in the negative direction, the single layer of point monopoles achieves perfect transmission with zero reflection and absorption as shown in Figure 4(b). Hence, this control source configuration still achieves nonreciprocal sound transmission at oblique angles of incidence. In the positive incident wave case, Figures 4(c) shows that the dual layer of point monopoles still minimise the transmitted and reflected wave components, and, thus, it maximises sound absorption of the incident sound field. However, when the incident wave is propagating in the negative direction, this control source configuration achieves near-perfect transmission with zero reflection and near-zero absorption. In the oblique incidence negative propagating wave case, the absorption controller only achieves near-perfect transmission because the reference signals, A, to the absorption controller in this case are nonzero, which leads to this controller minimising a proportion of the transmitted wave as shown in Figure 4(d). The reference signals, A, to the absorption controller in the oblique incidence case are greater in magnitude compared to the normal incidence negative case due to the extra phase shift applied to the pressure measured at each pressure sensor by weighting factors given by Eq. 4. The additional phase shift introduced by the weighting factors at each pressure sensor leads to a greater difference between the calculated total pressure and particle velocity at the midpoint between each pair of pressure sensors and, thus, the reference signals, A, for the absorption controller become nonzero. This also occurs in the transmitted wave controller at oblique incidence, however, in the negative incidence case, the

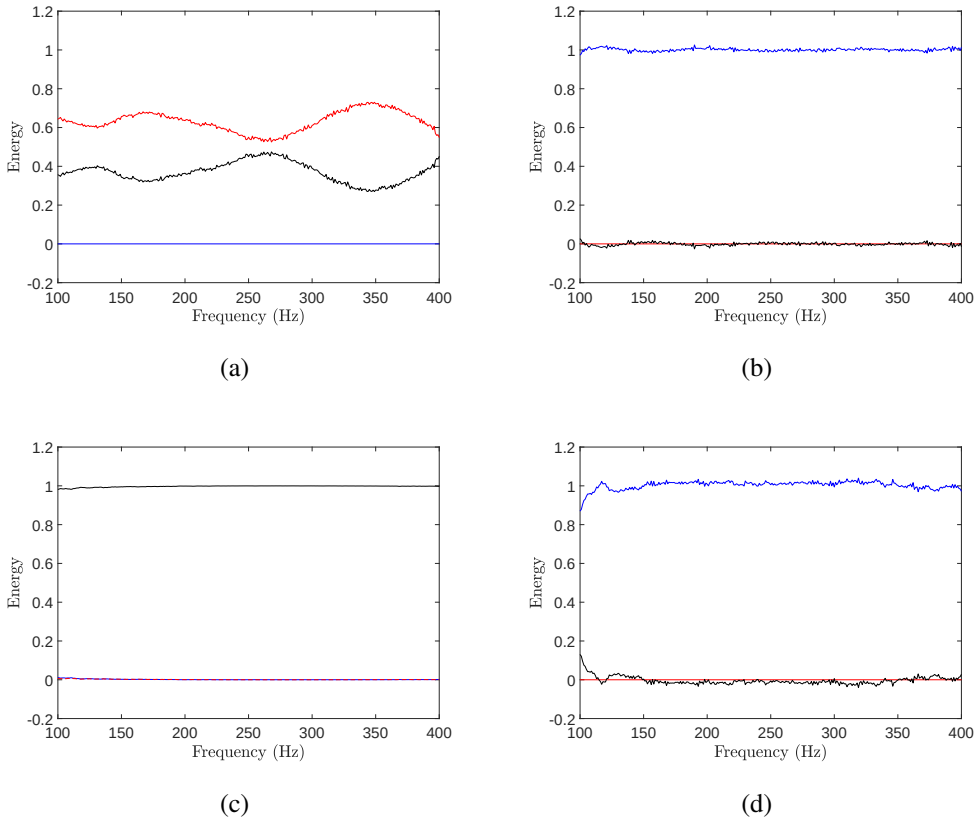

Figure 2: The performance of the array of single point monopole (a,b) and pairs of point monopole (c,d) control sources in terms of the average transmitted (blue), reflected (red) and absorbed (black) energy when a normal incident plane wave is propagating in the positive (a,c) and negative (b,d) directions.

transmitted wave controller minimises the reflected wave, C. Thus, Figures 4(c) and 4(d) show that the absorption controller described in Section 4 still has the ability to drive the dual layer of point monopole control sources to achieve nonreciprocal sound absorption at oblique angles of incidence, however, in the oblique incidence negative propagating wave case, the performance of the absorption controller is reduced compared to the normal incidence case due the wave separation method.

Similarly to the normal incident case, the contour plots showing the pressure field due to the oblique incidence positive propagating wave and the total sound field when implementing the proposed wave-based active control systems at 250Hz are shown in Figure 5. Figure 5(a) shows the oblique incidence positive propagating wave without control. Figure 5(b) shows that the transmitted wave controller still has the ability to minimise the sound transmission at oblique angles of incidence, however, the control sources still partly reflects the incident sound field, which generates a standing wave in the upstream section as shown in Figure 5(b). Figure 5(c) shows that the absorption controller still minimises the sound transmission, but leaves the upstream sound field before control unaffected due to the control of the reflected wave component.

6. CONCLUSIONS

There has been significant interest in the development of nonreciprocal acoustic devices that have the ability to block the incident waves propagating in one direction, whilst the incident waves propagating in the opposite direction are perfectly transmitted. Previously proposed nonreciprocal acoustic devices typically introduce nonlinearities, fluid motion or resonant cavities and these systems generally have performance limitations, which can limit their application. This paper has

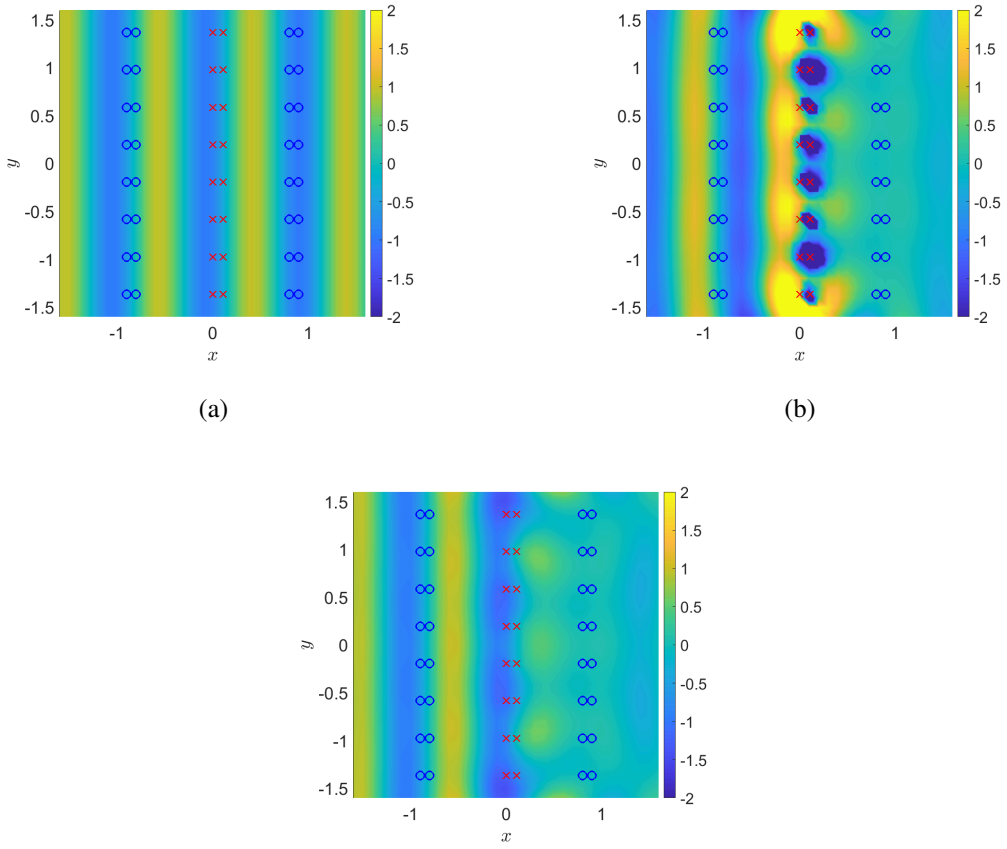

(a) (b)

(c)

Figure 3: The pressure contour plot of the normal positive propagating incident plane wave with no control (a), the total sound field when implementing the transmitted wave controller using a single layer of point monopole control sources (b) and the absorption controller using the dual layer of point monopole control sources (c) at 250Hz. The red crosses in each plot indicate the point monopole control sources and the blue circles in each plot indicate the pressure sensors.

investigated how active control can be used to control the transmitted and reflected wave components individually to achieve nonreciprocal sound transmission and absorption in a two-dimensional environment. Two different active control strategies have been proposed: a single layer of point monopole control sources that are driven to minimise the transmitted wave and a dual layer of point monopole control sources that are driven to minimise the transmitted and reflected waves, which results in absorption control.

The results presented in this paper have shown that the single layer of point monopole control sources achieves nonreciprocal sound transmission, whilst the dual layer of point monopoles achieves nonreciprocal sound absorption for both normal and oblique incident waves . Another advantage of the proposed wave-based active control systems is that they are fully adaptable and the direction of the nonreciprocal behaviour can be reversed. These active control systems provide further advancement in the development of fully adaptable linear nonreciprocal acoustic devices.

ACKNOWLEDGEMENTS

This research was partially supported by an EPRSC iCASE studentship (Voucher number: 17000146) and the Intelligent Structures for Low Noise Environments (ISLNE) EPSRC Prosperity Partnership (EP/S03661X/1).

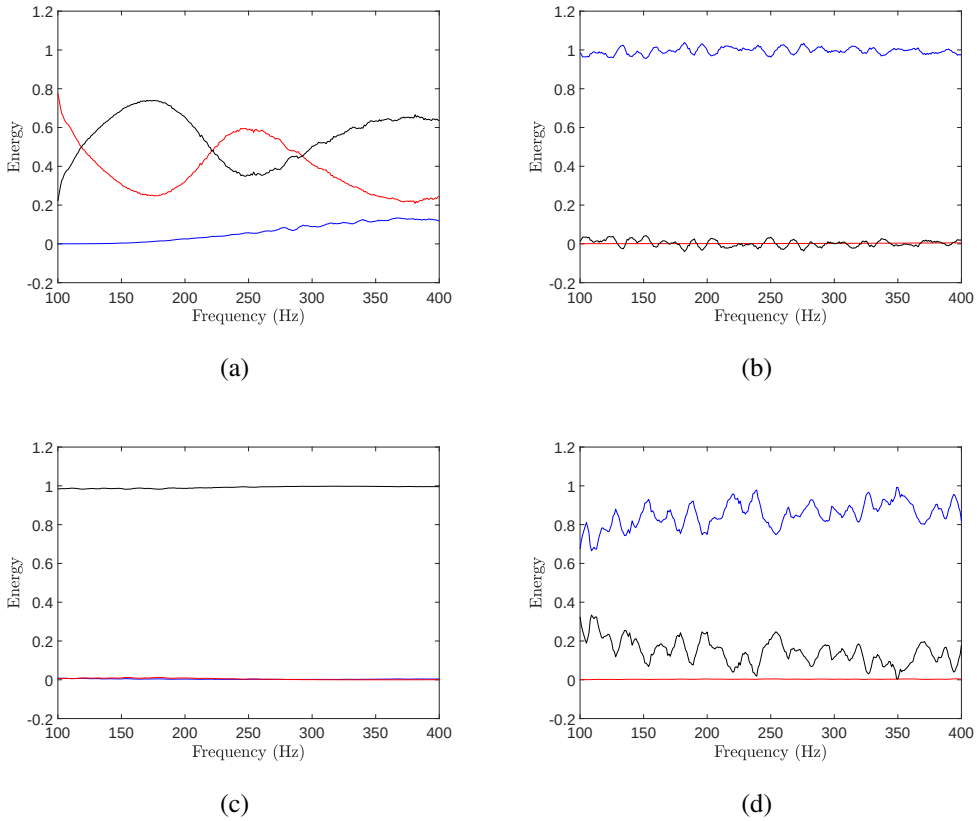

Figure 4: The performance of the array of single point monopole (a,b) and pair of point monopole (c,d) control sources in terms of the average transmitted (blue), reflected (red) and absorbed (black) energy when a 45° incident plane wave is propagating in the positive (a,c) and negative (b,d) directions.

REFERENCES

[1] Bogdan Ioan Popa and Steven A. Cummer. Non-reciprocal and highly nonlinear active acoustic metamaterials. *Nat. Commun.*, 5:3398, 2014.

[2] Chang Liu, Zongliang Du, Zhi Sun, Huajian Gao, and Xu Guo. Frequency-Preserved Acoustic Diode Model with High Forward-Power-Transmission Rate. *Phys. Rev. Appl.*, 3(6):064014, 06 2015.

[3] B. Liang, X. S. Guo, J. Tu, D. Zhang, and J. C. Cheng. An acoustic rectifier. *Nat. Mater.*, 9(12):989–992, dec 2010.

[4] Romain Fleury, Dimitrios L Sounas, Caleb F Sieck, Michael R Haberman, and Andrea Alù. Acoustic Circulator. *Science (80-.).*, 343(January):516–519, 2014.

[5] Romain Fleury, Dimitrios L. Sounas, and Andrea Alù. Subwavelength ultrasonic circulator based on spatiotemporal modulation. *Phys. Rev. B*, 91(17):174306, may 2015.

[6] Zhong-ming Gu, Jie Hu, Bin Liang, Xin-ye Zou, and Jian-chun Cheng. Broadband non-reciprocal transmission of sound with invariant frequency. *Sci. Rep.*, 6(1):19824, apr 2016.

[7] Amr Baz. Active nonreciprocal acoustic metamaterials using a switching controller. *J. Acoust. Soc. Am.*, 143(3):1376–1384, 2018.

[8] Efren Fernandez-Grande and Finn Jacobsen. Sound field separation with a double layer velocity transducer array (l). *The Journal of the Acoustical Society of America*, 130(1):5–8, 2011.

[9] Efren Fernandez-Grande, Finn Jacobsen, and Quentin Leclere. Sound field separation with sound pressure and particle velocity measurements. *The Journal of the Acoustical Society of*

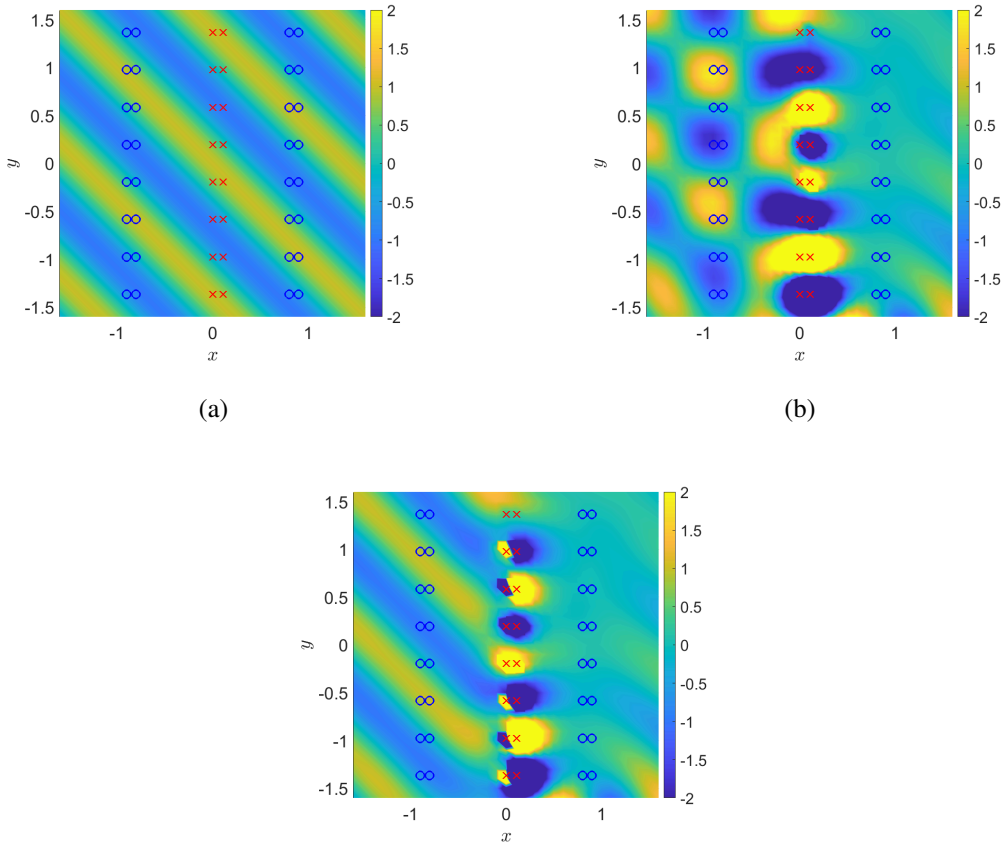

(a) (b)

(c)

Figure 5: The pressure contour plot of the 45° incident positive propagating plane wave with no control (a) and the total sound field when implementing the transmitted wave controller using a single layer of point monopole control sources (b) and the absorption controller using the dual layer of point monopole control sources (c) at 250Hz. The red crosses in each plot indicate the point monopole control sources and the blue circles in each plot indicate the pressure sensors.

America, 132(6):3818–3825, 2012.

[10] Masayuki Tamura. Spatial fourier transform method of measuring reflection coefficients at oblique incidence. i: Theory and numerical examples. *The Journal of the Acoustical Society of America*, 88(5):2259–2264, 1990.

[11] Masayuki Tamura, Jean F Allard, and Denis Lafarge. Spatial fourier-transform method for measuring reflection coefficients at oblique incidence. ii. experimental results. *The Journal of the Acoustical Society of America*, 97(4):2255–2262, 1995.

[12] H. Zhu, R. Rajamani, and K. A. Stelson. Active control of acoustic reflection, absorption, and transmission using thin panel speakers. *J. Acoust. Soc. Am.*, 113(2):852–870, 2003.

[13] John E Dennis Jr and Robert B Schnabel. *Numerical methods for unconstrained optimization and nonlinear equations*. 1996.

[14] CR Halkyard and BR Mace. Feedforward adaptive control of flexural vibration in a beam using wave amplitudes. *Journal of Sound and Vibration*, 254(1):117–141, 2002.